Monolithic IMPATT Oscillator Characterization

NAN-LEI WANG, MEMBER, IEEE, AND MICHAEL COBB

Abstract—**Recent interest in monolithic millimeter-wave IMPATT's has generated much activity. However, there have been few measurements to confirm circuit design predictions. Both the high-frequency and the low IMPATT impedance levels make such measurements difficult and inaccurate. In this paper, two useful methods for characterizing the resonator will be described. Theory and experiment will be presented.**

I. INTRODUCTION

MONOLITHIC IMPATT circuits will offer relatively high power in the millimeter-wave region. Their small size and light weight are important in many system applications as compared with the present waveguide circuitry. Both hybrid [1], [2] and monolithic [3], [4] microstrip circuits have been studied. These circuits, however, are often developed using computer-aided design methods without experimental verification of circuit element characteristics.

Circuit and device characterization is difficult in the millimeter-wave band. A particular problem is the necessary de-embedding of the circuit through the transition from waveguide to microstrip. The procedure [5] suffers from a lack of calibration standards and variations in sample assembly. The difficulty is compounded when measurements are made of matching structures required for IMPATT diodes. Such structures often have a reflection coefficient of 0.96 to 0.98 in a 50 Ω system. An accurate measurement would require a magnitude resolution of 0.01.

Since the total circuit resistance presented to the diode consists of the useful load resistance plus the resistance due to losses within the resonator, it is important to obtain a measurement of resonator Q. This will determine the "circuit efficiency," η_c, which is the ratio of the power reaching the output port to the power generated by the IMPATT diode. The resonator losses must be much lower than the negative resistance of the IMPATT in order to give a high circuit efficiency.

To address the measurement problems described above, two methods were developed to characterize the monolithic IMPATT resonator: 1) a transmission resonance method and 2) a varactor method. We have found these two methods useful in determination of the resonator loaded Q, unloaded Q, circuit efficiency, and matching impedance, as described in the following sections.

Manuscript received January 12, 1988; revised July 7, 1988.

The authors are with the Raytheon Research Division, 131 Spring St., Lexington, MA 02173.

IEEE Log Number 8824988.

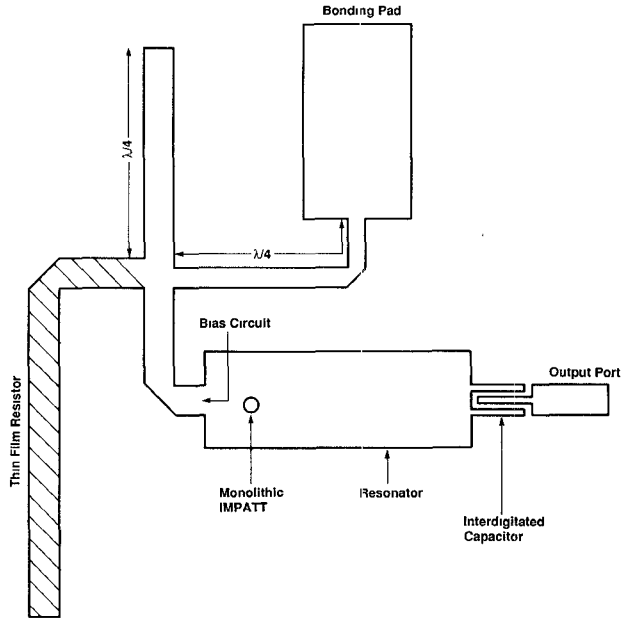

Fig. 1. Layout of a monolithic IMPATT oscillator with interdigitated capacitor as output coupling.

II. MONOLITHIC IMPATT OSCILLATOR DESIGN

A microstrip resonator design successfully used in a 44 GHz monolithic IMPATT oscillator [4] is shown in Fig. 1. An interdigitated capacitor was used as the output coupler. A section of low-impedance microstrip line forms the main body of the resonator. The monolithic IMPATT diode is connected in shunt through a via hole. On the other side of the diode is the dc bias and RF stabilization circuit, which presents an open circuit near the operation frequency and can be neglected in the calculation of the matching impedance. The requirement for oscillator design is that the load impedance be the negative of the diode impedance. In Fig. 2, the negative of the diode impedance at the frequency of interest has been generated by an analytical model [6] for specified doping and operational parameters. The impedance at several reference planes is also shown for the interdigitated capacitor resonator. Increasing the coupling capacitance increases the real part of the load impedance. The imaginary part is determined by the length of the 25 Ω line and the via hole inductance.

Microstrip line loss would result in an inward spiraling of the impedance on the Smith chart along the 25 Ω transmission line. The loss is not included in Fig. 2. Based on a microstrip line characterized result as discussed later,

0018-9480/89/0200-0393$01.00 ©1989 IEEE

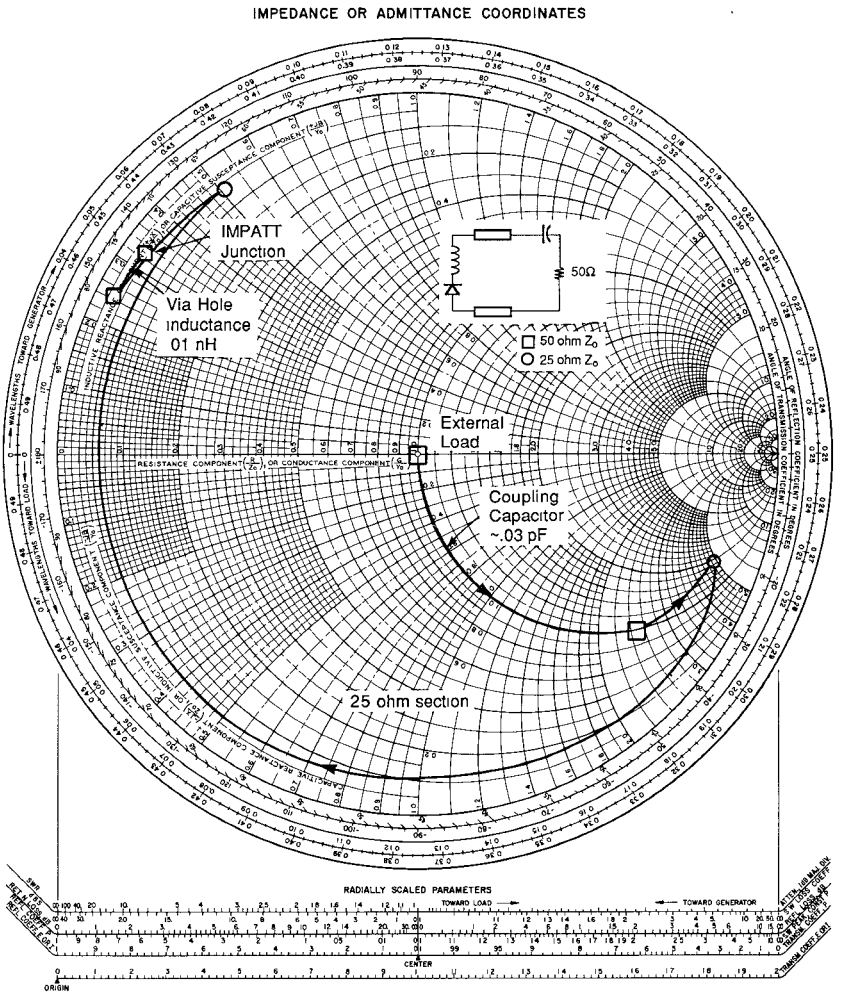

Fig. 2. Impedance transformation of the resonator design in Fig. 1.

it is estimated that a quarter-wavelength section will present a loss of about 0.1 Ω at the diode port. This is quite substantial compared with the negative resistance of an IMPATT device, which is a few tenths of an Ω.

The intrinsic loss of the coupler has an even more profound effect on the resonator circuit efficiency. For instance, if the Q factor of the interdigitated capacitor drops from infinity to 15, the circuit efficiency drops from 80 percent to 40 percent, according to the CAD simulation. Therefore, experimental verification of the design is crucial to the monolithic IMPATT oscillator optimization.

III. Transmission Resonance Method

One possible technique to obtain accurate characterization of the IMPATT circuit resonator is the use of "transmission resonance." Transmission resonance has been extensively used to measure the microstrip line parameters [7] at microwave frequencies where a half-wavelength section is lightly coupled on both ends. The transmission coefficient versus frequency is measured and the microstrip Q factor can be extracted. The light coupling gives minimum perturbation to the half-wavelength resonator. Microstrip line is characterized by this method and the result will be presented at the end of this section.

In the present case of resonator characterization, we construct a test pattern consisting of symmetrical back-to-back structures. Fig. 3 shows test patterns of three different resonator designs. From the test pattern, we can measure the resonator circuit efficiency, the resonator loaded Q, and the impedance at the input port of the resonator near the diode.[1]

In terms of the S parameters of the IMPATT resonator, the test pattern may be analyzed as shown in Fig. 4. The measured S parameters of the test pattern can be related to the resonator S parameters by the following equations, where the capital S is the parameter of the test pattern and the lowercase s represents the resonator:

$$S_{21} = \frac{s_{21}s_{12}}{1 - s_{22}^2} \tag{1}$$

$$S_{11} = s_{11} + \frac{s_{21}s_{12}s_{22}}{1 - s_{22}^2}. \tag{2}$$

The circuit efficiency of the oscillator is defined as the ratio of the power reaching the output port to the power

[1]In the paper, oscillator means the complete circuit with IMPATT diode for power generation. Resonator means the passive circuit matching the IMPATT diode. A test pattern is composed of two resonators connected in a back-to-back configuration.

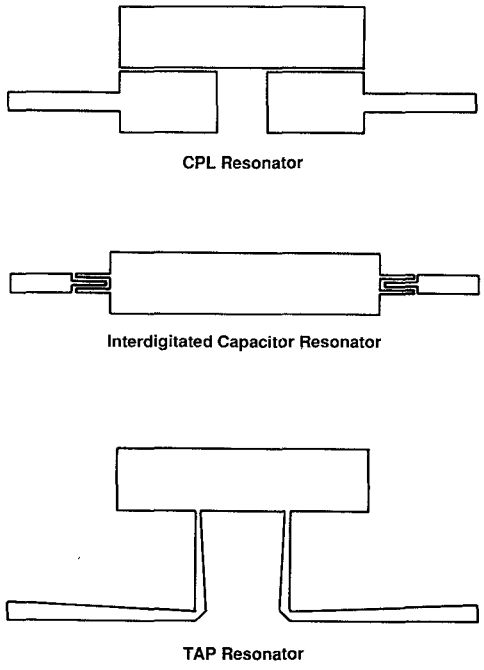

Fig. 3. Test patterns of the transmission resonance method. Three resonator designs are characterized this way.

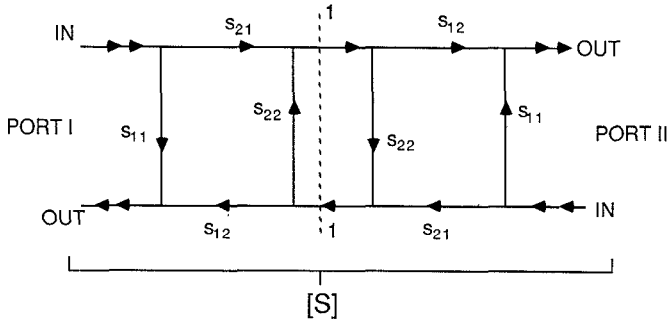

Fig. 4. S parameter representation of the test pattern in Fig. 3. The s (small letter) parameter represents the portion of the passive circuit in Fig. 5.

generated by the IMPATT. Mathematically it can be expressed by

$$\eta_c = \frac{|s_{21}s_{12}|}{1-|s_{22}|^2}. \tag{3}$$

Comparing (1) and (3), it is found that $|S_{21}| = \eta_c$ when s_{22} is real. Therefore, port 2 of the diode resonator in Fig. 5 is defined to be at the minimum of either voltage or current.

It can be formulated in another way. Near the resonance frequency, each IMPATT resonator can be modeled by a serial *RLC* circuit as shown in Fig. 6, with the reference plane (which is the central line in the figure) placed at the diode port. The coupling coefficient β of the test structure can be expressed as

$$\beta = R_L/2R_s \tag{4}$$

and the circuit efficiency of the resonator is

$$\eta_c = \frac{R_L}{R_L+R_s} = \frac{2\beta}{1+2\beta}. \tag{5}$$

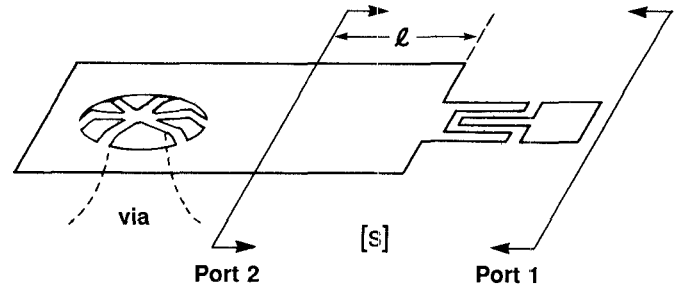

Fig. 5. The passive circuit that is characterized with the transmission resonance method is denoted here.

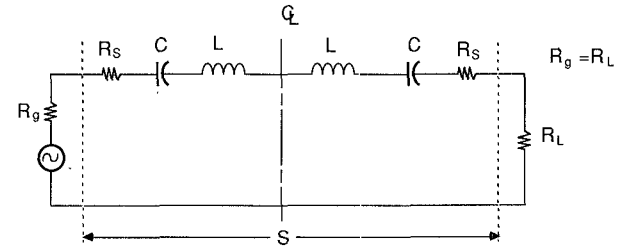

Fig. 6. *RLC* representation of the test pattern near resonance. The reference plane is now at the central line of the test pattern.

At resonance, the power transfer ratio [8] of the test pattern is

$$T(\omega_0) = |S_{21}|^2 = \frac{4\beta^2}{(1+2\beta)^2} = \left(\frac{R_L/R_s}{1+R_L/R_s}\right)^2 = \eta_c^2. \tag{6}$$

Therefore, it is concluded from (1) and (6) that at resonance $|S_{21}| = \eta_c$ and s_{22} is real.

In addition to the circuit efficiency, we may determine the loaded Q of the IMPATT resonator, Q_L, given by

$$Q_L = \frac{\omega L}{R_s+R_L} = \frac{\omega L}{R_s}\cdot\frac{1}{1+2\beta} = Q_0\cdot\frac{1}{1+2\beta} \tag{7}$$

where $Q_0 = \omega L/R_s$ is the unloaded Q of the resonator. For the test structure, the loaded Q is

$$Q'_L = \frac{\omega\cdot 2L}{2R_s+2R_L} = Q_L.$$

Therefore, the loaded Q of the IMPATT resonator can be determined by the measurement on the test structure. From a plot of $|S_{21}|$ versus frequency, the resonance frequency f_0 and the 3 dB bandwidth Δf can be determined. This gives $Q_L = f_0/\Delta f$ [8]. The unloaded Q of the resonator can be calculated from (5) and (7).

Finally, we can estimate the circuit impedance of the resonator at the IMPATT diode port. The following calculation is based on the assumption that the coupler has a negligible phase change with respect to frequency. Correction terms can be made when the phase of coupler versus frequency is known. Each type of output coupler has a different phase versus frequency function. The ports of the resonator are defined in Fig. 5 in relation to the planar IMPATT diode. The diode is connected to the resonator through a multistrap air bridge and a section of the 25 Ω

line, and to the ground plane of the microstrip through a via hole. Since s_{22} at the resonance frequency is real, the load impedance at port 2 is resistive. Let l be the distance along the resonator as shown in Fig. 5. At this distance, the phase of the rotation along the resonator is

$$\theta = \frac{l}{\lambda_g} \cdot 4\pi = 4\pi \cdot \frac{l\sqrt{k}\, f}{c} \tag{8}$$

where k is the effective dielectric constant and c is the light velocity in vacuum. Let $\rho = s_{22}$, the reflection at port 2 in Fig. 5. At resonance, ρ has a phase of 180°, and $\rho = \rho_r + j\rho_i$, $\rho_i \sim 0$. The impedance Z can be expressed as

$$Z = Z_0 \frac{1+\rho}{1-\rho}$$

$$\sim Z_0 \cdot \left(\frac{1+\rho_r}{1-\rho_r}\right)\left[1 - \frac{\rho_i^2}{1-\rho_r^2} + j\left(\frac{1}{1+\rho_r} + \frac{1}{1-\rho_r}\right)\rho_i\right]. \tag{9}$$

The reactance is

$$X = \mathrm{Im}(Z) = Z_0 \cdot 2\rho_i/(1-\rho_r)^2 \tag{10}$$

and

$$\rho_i = |\rho| \sin\phi \sim |\rho|(\pi - \phi) \tag{11}$$

where ϕ is the phase of s_{22}, and $\phi + \theta$ is a constant. The loaded Q can be related to the load impedance at port 2. The reactance X is expressed in (10), and R is the load resistance to be calculated:

$$Q_L = \frac{1}{2R} f_0 \cdot \frac{\partial X}{\partial f} = \frac{1}{2R} f_0 \cdot Z_0 \cdot \frac{2(-\rho_r)}{(1-\rho_r)^2} \cdot 4\pi \cdot \frac{l\sqrt{K}}{c} \tag{12}$$

since

$$\frac{\partial \rho_i}{\partial f} \sim |\rho|\left(-\frac{\partial \phi}{\partial f}\right) = |\rho|\frac{\partial \theta}{\partial f} = |\rho_r|_{\cdot\, \mathrm{at}\, f_0} 4\pi \cdot \frac{l\sqrt{K}}{c}$$

and for ρ_r near -1, $-\rho_r/(1-\rho_r)^2 \sim 0.25$

$$\therefore\ Q_L = 1/R \cdot Z_0 \cdot \pi \cdot l/\lambda g \tag{13}$$

and

$$R \sim 1/Q_L \cdot Z_0 \cdot \pi \cdot l/\lambda g. \tag{14}$$

A rotation on the Smith chart accounting for the microstrip section between port 2 and the diode will transform R in (14) to the impedance at the reference plane through the center of the diode and the via hole. The impedance presented to the IMPATT is the sum of the via hole inductance and the transformed impedance of R.

The test method described above was applied to the three resonator designs shown in Fig. 3. Input and output coupling to the microstrip sample was provided by a broad-band transition. The measured properties of a back-to-back pair of transitions are shown in Fig. 7. To a good approximation for the resonance method, the transitions can be represented as attenuators with a combined value of 1.2 dB.

As an example of the data, the measured $|S_{21}|$ for the interdigitated capacitor coupled resonator is shown in Fig. 8. For comparison, the figure also shows predicted results obtained with SuperCompact (trademark for Compact Engineering software). The transition jig is included in the computer file. Therefore, 1.2 dB has to be subtracted from the insertion loss at resonance for the calculation of the circuit efficiency. The ripple in the data is related to noise in the ANA system. The general agreement between calculation and measurement is good, but a discrepancy still exists. The difference results mainly from the smaller effective dielectric constant used in SuperCompact, and the model of interdigitated capacitor.

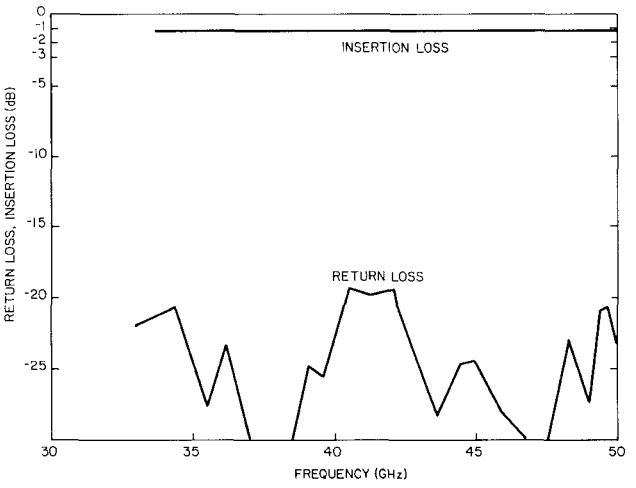

Fig. 7. Performance of Q-band ridge waveguide transition. Two transitions are connected in back-to-back configuration.

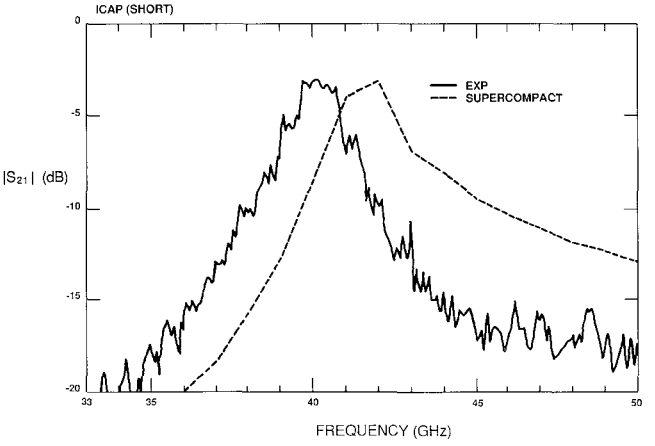

Fig. 8 Measured transmission of the test pattern with interdigitated capacitor, together with a simulation from SuperCompact. $f_0 = 40.33$ GHz, $\Delta f_{3\ \mathrm{dB}} = 1.77$ GHz, $S_{21} = -3$ dB, $\eta_c = 81.3$ percent.

Important parameters extracted from the data are summarized in Table I. For each resonator design, two patterns of slightly different length were tested. The impedance of the resonator microstrip line is 25 Ω. It is seen from the table that the circuit efficiency is generally around 80 percent with a load resistance less than 1 Ω. This is similar to design predictions. The loaded Q factor of these resonators is low, which is of advantage in the design of a wide-band IMPATT amplifier module.

It was noted earlier that in order to refer measured impedance levels to the reference plane of the IMPATT

TABLE I
SUMMARY OF THE TRANSMISSION RESONANCE CHARACTERIZATION

			fo GHz	R_L Ω	nc	Q_L	Δf GHz
CPL	long	exp 1	39.3	0.61	79.4%	26.58	1.48
		2	39.62	0.63	81.3%	26.23	1.51
		sc	40.6	0.9	80.2%	22.56	1.80
	short	exp	43.5	0.88	79.4%	18.67	2.33
		sc	44.1	1.0	82.4%	24.50	1.80
TAP	long	exp 1	41.2	2.23	86.1%	7.8	5.28
		2	40.86	2.53	86.1%	6.81	6.00
		sc	40.3	2.6	88.6%	6.72	6.00
	short	exp	44.85	1.09	78.5%	15.76	2.85
		sc	43.5	2.3	86.5%	8.53	5.10
ICAP	long	exp	35.9	0.63	79.4%	23.77	1.49
		sc	37.3	1.0	77.3%	24.87	1.50
	short	exp	40.33	0.63	81.3%	27.27	1.77
		sc	42.0	1.2	83.1%	16.15	2.60

CPL is the coupled line, TAP is the tap coupler, and ICAP is the interdigital capacitor.

SC is the CAD tool SuperCompact; exp denotes experimental data.

The value R_L in the experimental data is obtained by the equation $R_L \sim 1/Q_L \cdot Z \cdot \pi \cdot l/\lambda_g$. In SuperCompact it is calculated with the output end terminated.

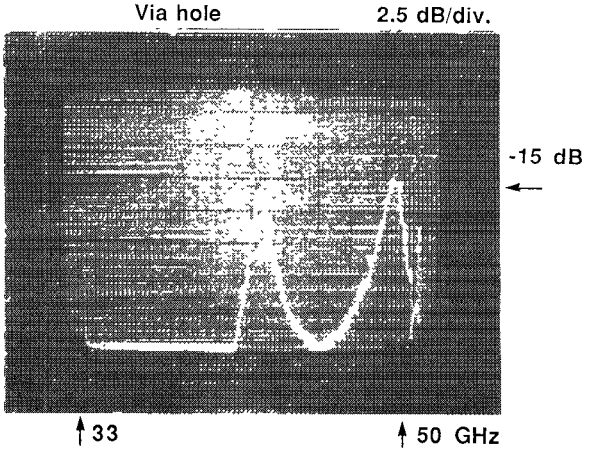

Fig. 9. Measured transmission of a via hole inductance embedded in a $\lambda/2$ microstrip resonator. The resonance peak at left is the one with via hole perturbation. The one on the right is the resonance of the $\lambda/2$ resonator with the via hole at the electrical short position.

diode, it is necessary to know the microstrip line electrical parameters and the effect of the via hole. This can also be obtained with the transmission resonance method.

Ordinary microstrip line on 0.004-in.-thick GaAs substrate is first characterized [7] in the frequency band of 33 to 50 GHz. The effective dielectric constant and the attenuation are obtained. Both 50 and 25 Ω lines were tested. The unloaded Q of the 25 Ω line is 115, slightly higher than that of the 50 Ω line.

The via hole inductance was characterized in the same way as in [9]. Fig. 9 shows measured values of $|S_{21}|$ versus frequency for a via hole embedded in a half-wavelength resonator. There are two resonance peaks. The higher

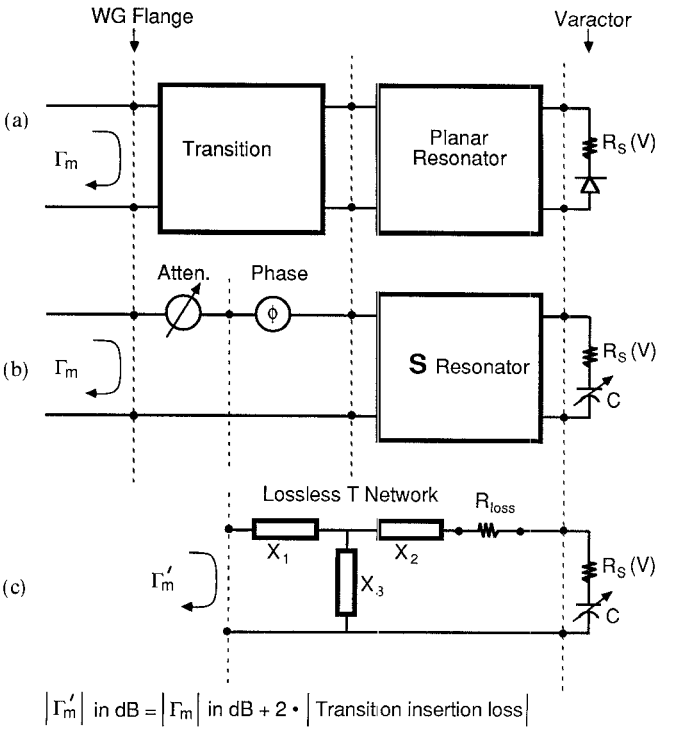

Fig. 10. Representation of the oscillator in the varactor method.

frequency peak corresponds to a half-wavelength resonance across the test structure. The via hole is located at an electric short location at resonance. This peak gives no information on via hole inductance. The lower frequency peak is the desired one. The shunt inductance of the via hole together with the microstrip section satisfies a resonance condition. With the known microstrip property, the via hole can be characterized as in [9]. The inductance thus characterized has a value of 10 pH and a series resistance of less than 0.1 Ω.

These data together with the resonator characterization result are sufficient to estimate the load impedance at the IMPATT diode.

IV. VARACTOR METHOD

The previous section outlined a technique for measurement of resonator properties based on a special test structure. A more direct method can be applied to planar IMPATT samples where only one port is accessible to the automatic network analyzer. The data are in the form of reflection coefficients at this port.

The IMPATT diode has a junction capacitance which is a function of bias voltage when the diode is biased below its breakdown voltage. As shown in Fig. 10, the IMPATT device used as a varactor can be modeled as a voltage-dependent serial RC circuit.

The transition and the resonator can be represented in two ways. The first representation is shown Fig. 10(b). Here the transition is represented by an attenuator and a phase shifter. This is a good approximation for a transition with very low or no reflection. The loss of the transition jig is absorbed into the measured reflection coefficient,

TABLE II
MEASURED REFLECTION COEFFICIENT OF THE MONOLITHIC IMPATT OSCILLATOR IN THE VARACTOR METHOD

Bias Voltage (v)	3.27	4	4.68	6	9.1	16
Capacitance (pF)	.69	.591	.49	.387	.29	.226
Magnitude of Γ	.735	.702	.633	.484	.518	.692
Phase of Γ	-49.3	-47.6	-45.4	-50.1	-79.7	-81.1

The reference plane is at the WG flange of the transition. The insertion loss of the transition is about 0.6 dB.

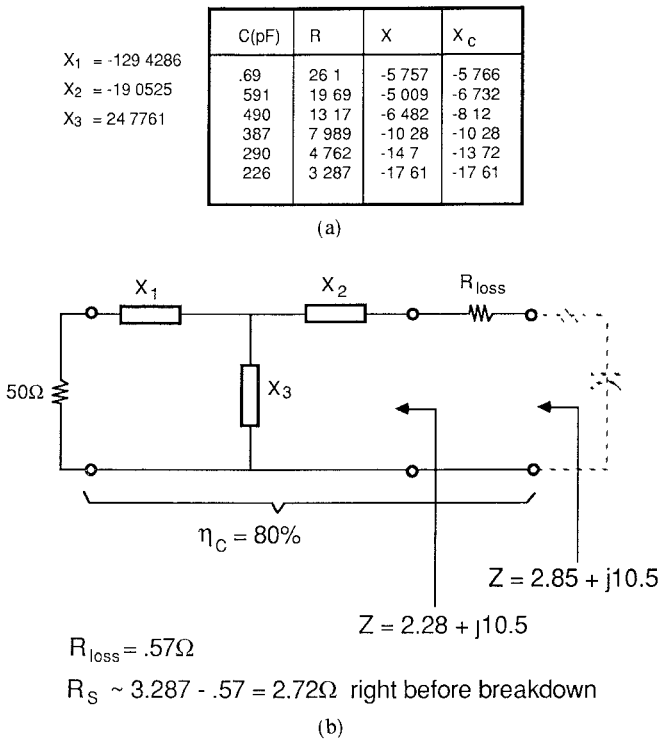

Fig. 11. Characterization with varactor method. The loss of the transition is removed from the measured reflection coefficient. (a) Characterization result of the oscillator with the IMPATT as a varactor. (b) The load impedance at diode port as derived from the result in (a).

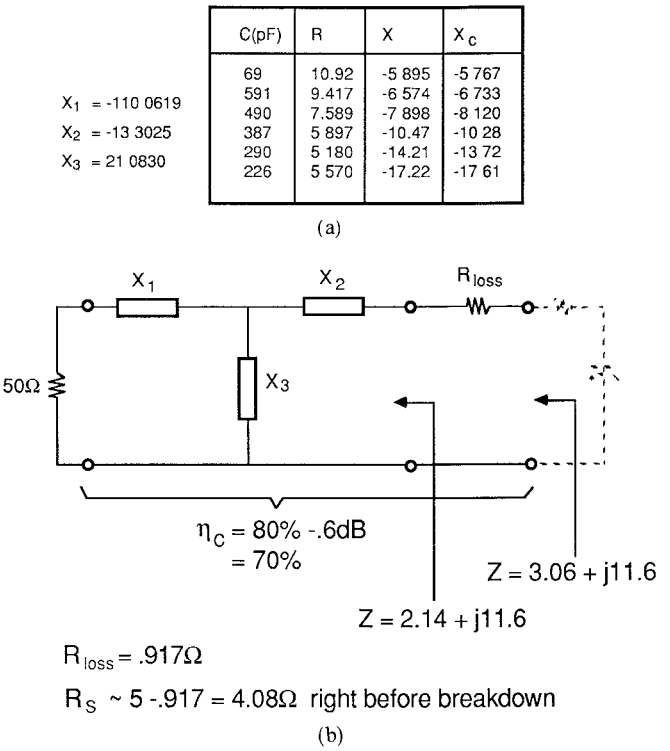

Fig. 12. Characterization with varactor method. The loss of the transition is included in the calculation. (a) Characterization result of the oscillator with the IMPATT as a varactor. (b) The load impedance at diode port as derived from the result in (a).

whereas the phase is absorbed into the resonator. The resonator is represented by a lossless T network and a series resistance, R_{loss}, as shown Fig. 10(c).

The second approach is to represent the transition and the resonator together by a lossless T network and a series resistance. Both methods should give the same load impedance at the diode port. The second approach is more suitable for a transition with higher reflection. In effect, the transition becomes part of the IMPATT resonator.

The reflection from the complete assembly is measured at three bias voltages. The capacitances at the three bias voltages are measured separately at low frequency. The reflection coefficient can be expressed in terms of the three T network reactances and the RC combination which has three unknown values of $(R_{\text{loss}} + R_s(V))$. There are three complex equations with six real unknowns, providing sufficient data to obtain a solution.

The test proceeds as follows: The diode junction capacitance versus bias voltage is measured at 1 MHz by first measuring the junction capacitance together with the static capacitance of the resonator. The diode is then disconnected from the resonator. This step leads to the destruction of the oscillator. The static capacitance of the resonator is measured and subtracted from the total capacitance to reveal the junction capacitance.

To separate R_{loss} from the total series resistance, the circuit efficiency characterized in the previous section must be used. In the first approach, where the transition loss is absorbed into the measured reflection coefficient, R_{loss} will be chosen so that the T network, including R_{loss}, will give the correct resonator circuit efficiency. The remaining resistance comes from the diode structure. For the second approach, where the transition and the resonator are treated as a network, the T network and the R_{loss} give a circuit efficiency which is the product of the resonator circuit efficiency and the transition loss. In either case, $R_{\text{loss}} = R \cdot (1 - \eta_c)/\eta_c$, where R is the load resistance transformed through the T network.

The reflection coefficient versus voltage locus will follow an arc on the Smith chart. Accuracy is related to the radius of curvature of the arc. When the arc defined by the measured reflection coefficients is small, calculation data become ill-conditioned and ANA measurement errors are magnified. Resonating the diode at or near the minimum varactor capacitance ensures a large radius of curvature on the Smith chart.

The varactor method was applied to a monolithic oscillator of poor performance since the method is destructive.

The ANA was calibrated to the waveguide test port, and the reflection from the oscillator was measured with the bias voltage below breakdown. The measured reflection coefficient is listed in Table II. Figs. 11 and 12 are the results of calculation. In Fig. 11, the loss of the transition is removed first, then the T network and total series resistance are calculated. Fig. 12 is a direct calculation where the series resistance includes the loss of the transition.

Figs. 11(b) and 12(b) present the T network components and the calculated matching impedance. The two methods give very good agreement in the diode port load impedance. As shown by this method, the poor performance of the circuits is caused by a large series resistance. The accuracy of the result is uncertain since the arc of the reflection coefficient is small. The R_s values are not as accurate since it is more sensitive to measurement errors.

V. Conclusion

Two methods were developed to characterize the monolithic IMPATT resonator used in the design of the millimeter-wave oscillators. Although they are only good for discrete frequency points, the accuracy is much better than the method of de-embedding. The transmission resonance method can also be applied to other circuitry with high reflection coefficients, such as the matching circuit of a narrow-band power FET, or HBT. The varactor method is very handy for *in situ* measurements. The drawback is that it is destructive and the accuracy deteriorates when the loss is high (a small arc). The experimental results are valuable for monolithic IMPATT oscillator design.

Acknowledgment

The authors would like to thank Dr. R. Pucel for his helpful discussion and to acknowledge the support of D. Masse and the careful review of the manuscript by Dr. M. G. Adlerstein. Thanks also go to W. Stacey and R. Brooks for the processing of the wafers.

References

[1] M. Dydyk, "EHF planar module for spatial combining," *Microwave J.*, pp. 157–174, May 1983.
[2] B. Bayraktaroglu and H. D. Shih, "High efficiency millimeter wave monolithic IMPATT oscillators," in *IEEE MTT-S Int. Microwave Symp. Dig.*, 1985, pp. 82–85.
[3] B. Bayraktaroglu, N. Camilleri, and S. A. Lambert, "Monolithic millimeter-wave IMPATT transmitter," presented at 11th Biennial Cornell Conf.
[4] N. Wang *et al.*, "Q-band monolithic GaAs IMPATT oscillator," in *Proc. 1987 IEEE GaAs IC Symp.*, pp. 143–146.
[5] R. A. Speciale, "A generalization of the TSD network analyzer calibration procedure, covering *n*-port scattering parameter measurements, affected by leakage errors," *IEEE Trans. Microwave Theory Tech.*, vol. MTT-25, pp. 1100–1115, Dec. 1977.
[6] H. Statz, R. A. Pucel, J. E. Simpson, and H. A. Haus, "Noise in gallium arsenide avalanche read diodes," *IEEE Trans. Electron Devices*, vol. ED-23, pp. 1075–1085, Sept. 1976.
[7] K. C. Gupta, R. Garg, and I. J. Bahl, *Microstrip Lines and Slot Lines*. Dedham, MA: Artech House, 1979.
[8] M. Sucher and J. Fox, *Handbook of Microwave Measurements*. New York: Polytechnic Press, vol. 2, ch. 8.
[9] R. E. DeBrecht, "Impedance measurements of microwave lumped elements from 1 to 12 GHz," *IEEE Trans. Microwave Theory Tech.*, vol. MTT-20, pp. 41–48, Jan. 1972.

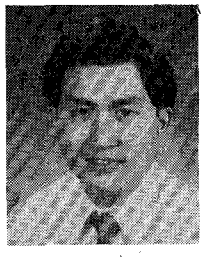

Nan-Lei Wang (S'82–M'85) was born in Taipei, Taiwan, Republic of China. He received the B.S. degree from National Taiwan University in 1979 and the M.S. and Ph.D. degrees from the University of California, Berkeley, in 1983 and 1985, respectively, all in electrical engineering. His Ph.D. thesis centered on a 35 GHz monolithic GaAs Gunn oscillator with coplanar waveguide matching circuit.

He joined the Raytheon Research Division in 1985. Between 1985 and 1987, he was responsible for the development of monolithic IMPATT technology. A Q-band IMPATT oscillator and an IMPATT VCO were demonstrated. At present, he is involved in device development and characterization for millimeter-wave MMIC. His major research interest is in high-power, high-frequency monolithic solid-state circuits.

Michael Cobb was born in Falkland, NC, on December 11, 1951. He received the B.S. degree in physics from East Carolina University in 1978. In 1983 he received the M.S. degree in microwave engineering from the University of Massachusetts under the UMASS/Raytheon MSEE Degree program.

He has been employed at the Raytheon Research Division since 1980, where he has performed dc and RF characterization measurements of pulsed X-band GaAs IMPATT diodes and circuits. Since 1983 he has been involved with the design, characterization, and simulation of millimeter-wave CW IMPATT oscillators and amplifiers.